REPORT DOCUMENTATION PAGE

Form Approved
OMB No. 0704-0188

1. AGENCY USE ONLY (Leave blank)	2. REPORT DATE	3. REPORT TYPE AND DATES COVERED
	January 12, 1996	Tech Rpt. # 26

4. TITLE AND SUBTITLE
Electric and Magnetic Behavior of $Ce_8Pd_{24}M$ Compounds with M = (Ga, In, Sn, Pb, Sb and Bi)

5. FUNDING NUMBERS
N00014-93-1-0904
Dr. John Pazik
R&T: 3134037ess08

6. AUTHOR(S)
R.A. Gordon, C.D.W. Jones, M.G. Alexander and F.J. DiSalvo

7. PERFORMING ORGANIZATION NAME(S) AND ADDRESS(ES)
Department of Chemistry
Cornell University
Ithaca, NY 14853-1301

8. PERFORMING ORGANIZATION REPORT NUMBER

9. SPONSORING/MONITORING AGENCY NAME(S) AND ADDRESS(ES)
Office of Naval Research
Chemistry Program
800 N. Quincy St.
Alexandria, VA 22217

10. SPONSORING/MONITORING AGENCY REPORT NUMBER

11. SUPPLEMENTARY NOTES

12a. DISTRIBUTION/AVAILABILITY STATEMENT
This document has been approved for public release and sale; its distribution is unlimited

12b. DISTRIBUTION CODE

13. ABSTRACT (Maximum 200 words)

We have prepared and examined the resistivity and magnetic susceptibility of a series of ternary compounds with composition $Ce_8Pd_{24}M$, where M is one of Ga, In, Sn, Sb, Pb or Bi and the related composition $La_8Pd_{24}In$. All members of this series are cubic with effective cerium moments consistent with tri-valent cerium. The lanthanum compound behaves as a simple metal in resistivity and has a small, negative susceptibility at 295K. All the cerium compounds but the gallide exhibit antiferromagnetic ordering below 10K. Metallic behavior is observed for all. The properties of the stannide, plumbide, antimonide and bismuthide reflect some weak interactions with crystal-field-split cerium states above 30K and changes in slope at low temperature coincident with the second-order antiferromagnetic phase transitions. Resistivities for the gallide and indide display broad features near 15K and 50K, respectively, suggesting a strong Kondo interaction is present in these materials.

14. SUBJECT TERMS	15. NUMBER OF PAGES
magnetic susceptibility, resistivity, Kondo effect, cerium intermetallic	30
	16. PRICE CODE

17. SECURITY CLASSIFICATION OF REPORT	18. SECURITY CLASSIFICATION OF THIS PAGE	19. SECURITY CLASSIFICATION OF ABSTRACT	20. LIMITATION OF ABSTRACT
Unclassified	Unclassified	Unclassified	

OFFICE OF NAVAL RESEARCH

Grant or Contract N00014-93-1-0904

R&T Code 3134037ess08
Scientific Officer: Dr. John Pazik

Technical Report No. 26

"Electric and Magnetic Behavior of $Ce_8Pd_{24}M$ Compounds with M = (Ga, In, Sn, Pb, Sb and Bi)"

b y

R.A. Gordon, C.D.W. Jones, M.G. Alexander and F.J. DiSalvo

Submitted to

Physica B

Cornell University
Department of Chemistry
Ithaca, NY 14853

January 12, 1996

Draft submitted 10/27/95

Electric and Magnetic Behavior of $Ce_8Pd_{24}M$ Compounds with M = (Ga, In, Sn, Pb, Sb and Bi)

R.A. Gordon, C.D.W. Jones, G. Alexander[1] and F.J. DiSalvo[2]
Department of Chemistry,
Cornell University, Ithaca, NY 14853-1301

To be submitted to Physica B

Abstract

We have prepared and examined the resistivity and magnetic susceptibility of a series of ternary compounds with composition $Ce_8Pd_{24}M$, where M is one of Ga, In, Sn, Sb, Pb or Bi and the related composition $La_8Pd_{24}In$. All members of this series are cubic with effective cerium moments consistent with tri-valent cerium. The lanthanum compound behaves as a simple metal in resistivity and has a small, negative susceptibility at 295K. All the cerium compounds but the gallide exhibit anti-ferromagnetic ordering below 10K. Metallic behavior is observed for all. The properties of the stannide, plumbide, antimonide and bismuthide reflect some weak interactions with crystal-field-split cerium states above 30K and changes in slope at low temperature coincident with the second-order anti-ferromagnetic phase transitions. Resistivities for the gallide and indide display broad features near 15K and 50K, respectively, suggesting a strong Kondo interaction is present in these materials.

Keywords: magnetic susceptibility, resistivity, Kondo effect, cerium intermetallic

---

[1] current address: Dept. of Physics, Seton Hall University, South Orange, NJ 07079

[2] corresponding author

1. Introduction

In cerium containing intermetallics, interaction between the 4f electron on a cerium atom and conduction electron states is influenced by the chemical environment around the cerium and by the separation between the Fermi level and the 4f energy level [1-4]. If the energy seperation is small, and if neighbouring atom conduction states favour strong interaction (hybridisation) with the 4f electron, then an intermediate valent state of the cerium may occur. This does happen in $CePd_3$, where extensive hybridisation due to a Kondo interaction has produced a non-integral cerium moment which becomes screened out as a result of the Kondo interaction below 135K [5]. However, upon incorporating some smaller P-block elements, B, Si, and Ge, into the body-centre interstitial site of $CePd_3$ as $CePd_3M_x$, the lattice expands without any observed distortion away from a simple defect perovskite structure, causing a loss of the IV state and a return to a full tri-valent cerium moment [6-8] with anti-ferromagnetic ordering for Si ($x = 0.3$, T_N=2.8K) and Ge ($x = 0.25$, $T_N = 3.2$K) [8].

Recently, we identified a ternary structure involving Ce, Pd and Sb that is closely related to the Cu_3Au structure of $CePd_3$ [9]. Instead of a simple occupation of the body-centre site to produce a perovskite-like material, the incorporation of 1 antimony per 8 $CePd_3$ units produces an ordered compound, $Ce_8Pd_{24}Sb$ (Fig. 1). Here, the Sb incorporated in the centre of a $CePd_3$ unit pushes the Pd atoms outward from the faces of the cube defined by the cerium atoms, resulting in a doubling of the lattice constant. The cerium remains co-ordinated by 12 palladium atoms at distances ranging from 2.97Å to 3.05Å (versus 2.92Å in $CePd_3$). Antimony is the next-nearest neighbour at a distance of 3.68Å, some 22% further away than the palladium atoms. We have succeeded in preparing isotypic variants of this structure by incorporating Ga, In, Sn, Pb

and Bi in place of Sb to explore the effects of small changes in electron count and interstitial atom size while keeping the local co-ordination environment of the cerium invariant.

2. Experimental

Samples were prepared by arc-melting elements of at least 99.9% purity in the desired ratio plus a small ($\lesssim$ 2%) excess of the more volatile Pb, Sb and Bi. Arc-melting was done on a tantalum-coated, water-cooled copper hearth under flowing titanium-gettered argon. Each sample was turned over and re-melted at least three times in an effort to produce homogeneous ingots. Mass losses after arc-melting were within 1% of the anticipated stoichiometric values. Samples were subsequently placed in sections of tantalum tubing, sealed in evacuated quartz tubes and annealed for two weeks at 900°C.

Powder diffraction data were collected using a SCINTAG θ-2θ diffractometer and Cu Kα1 radiation to check the single-phase nature of each sample. The diffraction patterns were indexed using the program TREOR90 [10] and the lattice constants obtained thereby were refined by a least-squares technique. The intensities and distribution of peaks in the powder diffraction patterns were comparable to those observed for $Ce_8Pd_{24}Sb$ [9].

Magnetic susceptibility measurements were performed by the Faraday method. Susceptibility data was fit to a Curie-Weiss expression, $\chi = \chi_o + C/(T - \theta)$, as described elsewhere [11]. Resistivity measurements were done in a 4-probe manner on rectangular sections of typical dimensions 7.0mm x 3.5mm x 1.1mm cut by string saw from larger ingots. Indium contacts were soldered on in most cases using an ultra-sonic soldering iron. The antimonide exhibited a tendency to crack on cooling when contacts were soldered on, so resistivity was

measured on it using 4 spring-loaded gold pins tipped with indium for better contact. No cracking occurred on cooling to 4.2K when this was done.

3. Results and Discussion

All samples are stable in air, with a freshly cleaved surface remaining silvery and highly reflective for timescales greater than 1 month in air. The plumbide and bismuthide are more brittle than the others but all could be ground under acetone for x-ray work. The lattice parameter and magnetic data for each of the $Ce_8Pd_{24}M$ compounds and $La_8Pd_{24}In$ are summarised in Table 1. The magnitudes of the resistivities at room temperature are roughly 10^{-4} Ω•cm, typical for an intermetallic containing transition elements and, indeed, comparable to that for $CePd_3$ [5].

$Ce_8Pd_{24}Sb$

After observing anti-ferromagnetic ordering in the other members of this series of compounds, it became apparent that insufficient data (Fig. 2a) had been collected below 50K for our previous conclusion of no ordering [9] to be completely valid. A second sample was prepared which did exhibit anti-ferromagnetic ordering (Fig. 2b), but this sample exhibited a 5% impurity in its powder diffraction pattern that belongs to a cubic phase (a = 8.593Å) we have observed in more Sb-rich compositions but have been unable to isolate. A third sample was prepared which appeared single phase by powder diffraction yet exhibited low temperature magnetic behavior (Fig. 2c) intermediate between samples (a) and (b). Details of the individual

sample preparations are given in Table 2. Sample (a) deviates the most from the ideal stoichiometric mass. Sample (b) contains an impurity phase and so may have lost Ce or Pd rather than Sb. Sample (c) would appear to be the sample of highest quality, but exhibits more complicated magnetic ordering than sample (b) with possibly three second order transitions signified by abrupt changes in slope (Fig. 3). Behavior similar to that observed in sample (c) has been observed in the susceptibility of $CePd_2Al_3$ [12] and was attributed to either an impurity or some possible incommensurate magnetic ordering.

Figure 4 shows the inverse magnetic susceptibility for sample (c) from 4.2K to 320K. The high temperature behavior ($T > 100K$) is consistent with that previously reported [9] with an effective cerium moment of $2.46(3)\mu_B$, which is slightly reduced from the Ce^{+3} free ion value of $2.54\mu_B$, and a Weiss constant, θ, of -11(2)K suggesting that there are indeed anti-ferromagnetic interactions present. However, θ cannot be interpreted as purely an exchange energy since it may have a contribution from a crystal field splitting energy [11]. Deviations from Curie-Weiss behavior below 100K can be attributed to temperature dependence of the occupation of a crystal field split $4f^1$ state. The resistivity (Fig. 5) also exhibits deviations (gradually increasing slope) below 100K that result from crystal field effects. A sharp drop in resistivity occurs below 6.5K, consistent with the initial transition observed at 6.4K in susceptibility (Fig. 4), where the onset of ordering produces a rapid reduction in magnetic scattering of conduction electrons. In light of the variable magnetic behavior, we are hesitant to claim no Kondo behavior is present, but there is no feature in the resistivity that could be ascribed to such an effect.

$Ce_8Pd_{24}Bi$

The behavior of the bismuthide mirrors the antimonide in most aspects (Fig. 6). Consistent with having a larger covalent radius (1.46Å) than Sb (1.40Å) [13], the cell constant is also slightly larger (Δa = 0.015Å) for the Bi-containing compound. As with the antimonide, the susceptibility for $Ce_8Pd_{24}Bi$ shows tri-valent behavior of the cerium atoms with an effective moment per cerium of 2.49(3)μ_B and anti-ferromagnetic exchange with θ = -11(2)K. Anti-ferromagnetic ordering is observed at 5K. Resistivity measurements (Fig. 7) also exhibit a broad roll-over on cooling from thermal depopulation of cerium 4f crystal field levels and a decrease near 5K consistent with the magnetic ordering temperature. The RKKY interaction [14], which can result in magnetic ordering if no direct exchange between moments is present, decreases in strength as (Ce-Ce separation)$^{-3}$. The lower Néel temperature in the bismuthide (5K versus 6K of sample (b) of the antimonide) correlates with a larger Ce-Ce distance in a cell with larger lattice constant.

$Ce_8Pd_{24}Sn$

The highest magnetic ordering temperature of this series occurs in $Ce_8Pd_{24}Sn$ with T_N = 7.5K (Fig. 8). The effective cerium moment of 2.49(4)μ_B and θ of -11(3)K are consistent with the above two compounds; tri-valent cerium with anti-ferromagnetic exchange. The resistivity (Fig. 9) also behaves in a similar manner with metallic behavior, weak crystal field interaction and a second order transition at 7.5K. Again, incorporating one Sn in 8 $CePd_3$ cells has resulted in an apparent loss of any appreciable Kondo interaction. A decrease of 1 electron from the antimonide has resulted in an increase in the Néel temperature.

$Ce_8Pd_{24}Pb$

As with the above 4 compounds, the resistivity of the plumbide (Fig. 10) exhibits a broad feature above 25K that can be described as a gentle roll-over in resistivity. Again, we associate this feature with the interaction between conduction electrons and cerium 4f electrons whose states have been split by interaction with a crystal electric field and the occupation of whose states varies with temperature when the temperature is comparable to the splitting energy. An abrupt decrease in resistivity below 6K coincides with the observed anti-ferromagnetic ordering in the magnetic susceptibility (Fig. 11). The high temperature susceptibility ($T > 80K$) can be fit to a Curie-Weiss expression with an effective moment per cerium of $2.48(3)\mu_B$ and a Weiss parameter of -10(2)K. The lower Néel temperature of 6K versus 7.5K in the stannide again correlates with the larger size of the interstitial Pb atom (covalent radius 1.47Å) compared to the size of Sn (1.40Å), as with the Sb/Bi relationship discussed above.

$Ce_8Pd_{24}Ga$

With a covalent radius of 1.26Å, gallium is the smallest atom we have incorporated at the 8:24:1 stoichiometry to produce this ordered variant. Germanium, with a radius of 1.22Å, is reported to occupy the body-centre site in $CePd_3$ as a perovskite-like material with no super-structural ordering [8]. Our results suggest, however, that a careful study of the 8:24:1 composition with B, Al, C, Si and Ge may reveal this ordered phase as well. Magnetic susceptility measurements on $Ce_8Pd_{24}Ga$ (Fig. 12) suggest a effective moment of $2.42(2)\mu_B$ per cerium ($T > 100K$) at high temperature and anti-ferromagnetic interactions ($\theta = -13(2)$). A moment of $2.42(2)\mu_B$ is noticeably lower than the free ion value of $2.54\mu_B$ but within the realm

of tri-valent behavior. Below 100K, as in the previous compounds, a gradual decrease in the slope of χ^{-1} occurs with decreasing temperature that may be due to crystal field effects. The inverse susceptibility appears to plateau below 7K, with the magnetic susceptibility achieving a value of 6.09×10^{-5} emu/g at 4.2K. The resistivity of $Ce_8Pd_{24}Ga$ (Fig. 13) shows a strong increase as the temperature decreases below 100K, reaching a maximum near 14K before dropping off. Similar behavior is observed in $CeFe_{0.53}Ge_2$ [15] and was attributed to a significant Kondo interaction.

On changing from group 15 through 14 to group 13 elements, several factors change: the size of the main group element, the energy of the p-block element contributions to the valence bands and the total electron count. The smaller size of Ga compared to Sn or Sb has resulted in a smaller cell (8.4078Å versus 8.4446Å) possibly allowing some marginally better overlap with the Ce 4f orbitals (shorter near-neighbour distances). We have already noted the effect on the Néel temperature for substituting a larger p-block element in group 14 and group 15-containing compounds for a smaller change (albeit increase) in the lattice constant. The major effect in this case is most likely the decrease of 1 electron from the stannide to bring the Fermi level closer to the 4f level relative to the stannide. An interaction which scales as the inverse of the energy separation between ϵ_f and ϵ_{Fermi}, like the Kondo interaction [16], would then be enhanced. How much of an enhancement would also depend on the density of conduction states, $D(\epsilon)$, near the Fermi level. For a slowly varying $D(\epsilon)$ near ϵ_F, the change in energy separation ($\epsilon_f < \epsilon_F$) could be expect to vary as $\Delta(\epsilon_F - \epsilon_f) \sim -1/D(\epsilon_F)$ for a decrease of 1 electron. This change in energy separation would then be large if $D(\epsilon_F)$ is small.

$Ce_8Pd_{24}In$ and $La_8Pd_{24}In$

Anti-ferromagnetic ordering occurs in $Ce_8Pd_{24}In$ near 4K (Fig. 14). There is potentially another second order transition at 7K in suceptibility and resistivity (Fig. 15) but its existence is not as apparent as those in the antimonide (sample (c)). Above 100K, the susceptibility can be fit to a Curie-Weiss expression to give an effective high temperature ($T > 100K$) moment of $2.43(2)\mu_B$/Ce, reduced, like the gallide compound, but within the realm of tri-valent cerium behavior. Some deviation in χ^{-1} below 100K (decreasing slope) may be attributed to some weak crystal field interaction but the resistivity (Fig. 15) does not corroborate this. The broad feature above 50K, with rapid drop-off below 50K does not resemble the gradual roll-over possessed by the resistivity of the stannide shown in Fig. 8 or that of the antimonide shown in Fig. 4. Nor does it resemble closely the peak in the resistivity for the Ga-containing compound, but we believe that it has a similar origin, a strong Kondo interaction. Similar curve shapes for resistivity and susceptibility are observed for the heavy fermion compound $CePd_2Al_3$ [12], albeit with the features at lower temperatures than in $Ce_8Pd_{24}In$.

The lanthanum version of this material possesses a susceptibility of $-2.8(3) \times 10^{-7}$ emu/g (Table 1), small and negative. This suggests a small density of conduction electron states, $D(\epsilon)$; a Pauli paramagnetic contribution to χ smaller than the core diamagnetism. If $D(\epsilon)$ is small in all these 8-24-1 materials, then the effect of losing 1 electron would lower the Fermi level an appreciable amount, increasing the strength of the 4f-conduction electron coupling [16].

4. Conclusions

We have prepared and examined the magnetic and electric behavior of a series of compounds of composition $Ce_8Pd_{24}M$ with M = {Ga, In, Sn, Pb, Sb, Bi} and $La_8Pd_{24}In$. From the small and negative room temperature magnetic susceptibility of the lanthanum compound, we infer a low density of conduction states in these materials: small changes in electron count could then have a large effect on the Fermi level and hence the separation between the Fermi level and the 4f energy level. Changing the electron count in 1 electron steps in moving from the group 15 to group 13 p-block elements we see a transition from anti-ferromagnetic ordering of tri-valent cerium moments and weak crystal field interactions to strong Kondo interactions, with $Ce_8Pd_{24}In$ exhibiting both types of behavior.

5. Acknowledgements

This work was supported by the Office of Naval Research and by the National Sciences and Engineering Research Council of Canada for a fellowship to C.D.W.J.

6. References

[1] F. Canepa, M. Minguzzi, G.L. Olcese, J. Magn. Magn. Mater. 63&64 (1987) 591.

[2] R.A. Neifeld, M. Croft, T. Mihalisin, C.U. Segre, M. Madigan, M.S. Torikachvili, M.B. Maple, L.E. DeLong, Phys. Rev. B 32 (1985) 6928.

[3] Z. Fisk, J.D. Thompson, H.R. Ott, J. Magn. Magn. Mater. 76&77 (1988) 637.

[4] F. Steglich, C. Geibel, K. Gloos, G. Olesch, C. Shank, C. Wassilew, A. Loidl, A. Krimmel, G.R. Stewart, J. Low Temp. Phys. 95 (1994) 3.

[5] P.A. Veenhuizen, Yang Fu-ming, H. van Nassou, F.R. de Boer, J. Magn. Magn. Mater. 63&64 (1987) 567.

[6] S.K. Dhar, S.K. Malik, R. Vijayaraghavan, Mat. Res. Bull. 16 (1981) 1557.

[7] S.K. Malik, S.K. Dhar, R. Vijayaraghavan, Pramana 22 (1984) 329.

[8] J.P. Kappler, M.J. Besnus, P. Lehmann, A. Meyer, J. Sereni, J. Less Common Met. 111 (1985) 261.

[9] R.A. Gordon, F.J. DiSalvo, Z. Naturforsch. 50b, in press.

[10] P.E. Werner, L. Eriksson, M. Westdahl, J. Appl. Crystallogr. 18 (1985) 367.

[11] R.A. Gordon, Y. Ijiri, C.M.Spencer, F.J. DiSalvo, J. Alloys Comp. 124 (1995) 101.

[12] H. Kitazawa, C. Schank, S. Thies, B. Seidel, C. Geibel, F. Steglich, J. Phys. Soc. Japan 61 (1992) 1461.

[13] R.T. Sanderson, Inorganic Chemistry, Reinhold Publishing Corporation, New York, 1967, 74.

[14] Ziman, J.M., Principles of the Theory of Solids (2nd Edition), Cambridge (1972), chapters 7 & 10.

[15] I. Das, E.V. Sampathkumaran, Solid State Comm. 83 (1992) 765.

[16] P.A. Lee, T.M. Rice, J.W. Serene, L.J. Sham, J.W. Wilkins, Comments Cond. Mat. Phys. 12 (1986) 99.

Table 1. Summary of cell and magnetic data.

$Ln_8Pd_{24}M$	a/Å	μ/μ_B	θ/K	T_N/K	fit range/K
$Ce_8Pd_{24}Sb$	8.4445(8)	2.46(3)	-11(2)	see Table 2	100 - 320
$Ce_8Pd_{24}Bi$	8.4601(8)	2.49(3)	-11(2)	5	80 - 310
$Ce_8Pd_{24}Sn$	8.4446(8)	2.49(4)	-11(3)	7.5	100 - 320
$Ce_8Pd_{24}Pb$	8.4605(8)	2.48(3)	-10(2)	6	80 - 310
$Ce_8Pd_{24}Ga$	8.4078(8)	2.42(2)	-13(2)	----	100 - 320
$Ce_8Pd_{24}In$	8.4457(8)	2.43(2)	-7(2)	4, 7	100 - 310
$La_8Pd_{24}In$	8.4940(8)	χ(295K) = -2.8(3) $\times$ 10^{-7} emu/g			

Table 2. Antimony excess (%), arc-melted mass data, magnetic moments and transition temperatures for 3 prepared $Ce_8Pd_{24}Sb$ samples.

Sb sample	Excess Sb/%	Final mass/g	Ideal mass/g	% of ideal	μ_{eff}/μ_B	Transition Temperature/K
(a)	1.5	1.8896(2)	1.9086	99.00	2.45(4)	---
(b)†	0.0	1.4043(2)	1.4082	99.72	2.51(3)	6.0
(c)	0.7	1.3664(2)	1.3668	99.97	2.46(3)	6.4, 5.7, 5.1

† possesses 5% impurity in powder diffraction pattern

Figure Captions

Figure 1. Perspective view of the cystal structure of $Ce_8Pd_{24}Sb$. Black Sb atoms mark the corners of the unit cell and Pd-Pd bonds are drawn to emphasise the distortions leading to the superstructure.

Figure 2. Inverse magnetic susceptibilities below 50K for $Ce_8Pd_{24}Sb$ samples having (a) 99% the anticipated stoichiometric mass, (b) 99.72% and (c) 99.97% after arc-melting.

Figure 3. Magnetic susceptibility of $Ce_8Pd_{24}Sb$ sample (c) below 10K. Arrows indicate possible second order phase transitions.

Figure 4. Inverse magnetic susceptibility of $Ce_8Pd_{24}Sb$ sample (c) from 4.2K to 320K. The magnetic susceptibility from 4.2K to 30K is shown in inset.

Figure 5. Resistivity of $Ce_8Pd_{24}Sb$ sample (c) from 4.2K to 300K.

Figure 6. Inverse magnetic susceptibility of $Ce_8Pd_{24}Bi$ from 4.2K to 320K. The magnetic susceptibility from 4.2K to 30K is shown in inset.

Figure 7. Resistivity of $Ce_8Pd_{24}Bi$ from 4.2K to 300K.

Figure 8. Inverse magnetic susceptibility of $Ce_8Pd_{24}Sn$ from 4.2K to 320K. The magnetic susceptibility from 4.2K to 30K is shown in inset.

Figure 9. Resistivity of $Ce_8Pd_{24}Sn$ from 4.2K to 300K.

Figure 10. Resistivity of $Ce_8Pd_{24}Pb$ from 4.2K to 300K.

Figure 11. Inverse magnetic susceptibility of $Ce_8Pd_{24}Pb$ from 4.2K to 320K. The magnetic susceptibility from 4.2K to 30K is shown in inset.

Figure 12. Inverse magnetic susceptibility of $Ce_8Pd_{24}Ga$ from ~~4.2~~ 2.4K to 320K.

Figure 13. Resistivity of $Ce_8Pd_{24}Ga$ from ~~4.2~~ 2.4K to 300K.

Figure 14. Inverse magnetic susceptibility of $Ce_8Pd_{24}In$ from 4.2K to 320K. The magnetic susceptibility from 4.2K to 30K is shown in inset.

Figure 15. Resistivities of $Ce_8Pd_{24}In$ and $La_8Pd_{24}In$ from 4.2K to 300K.

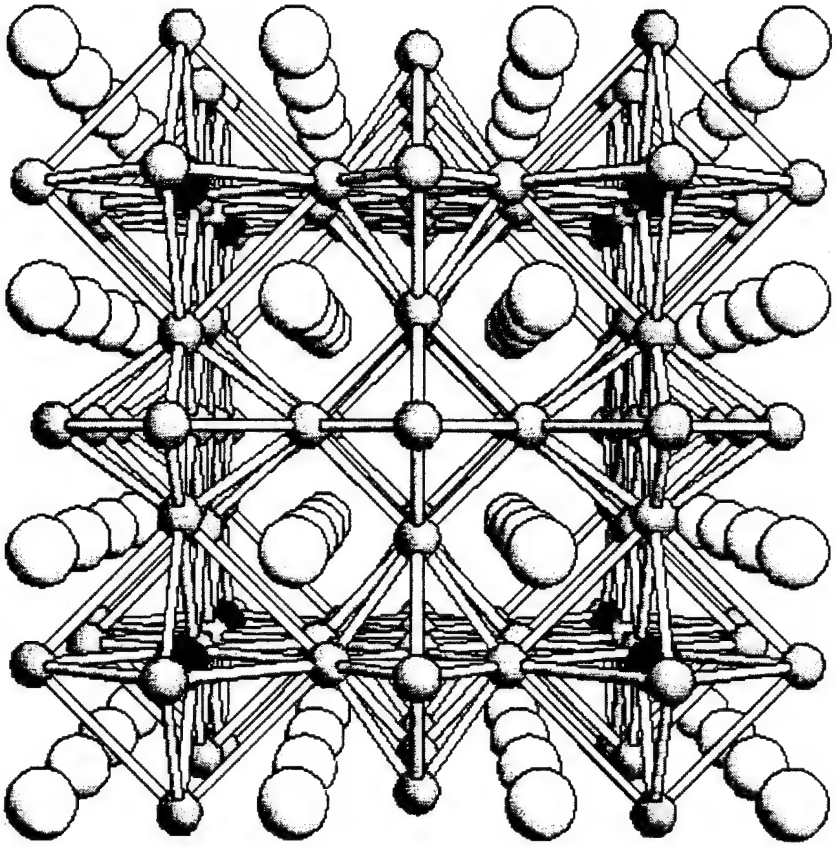

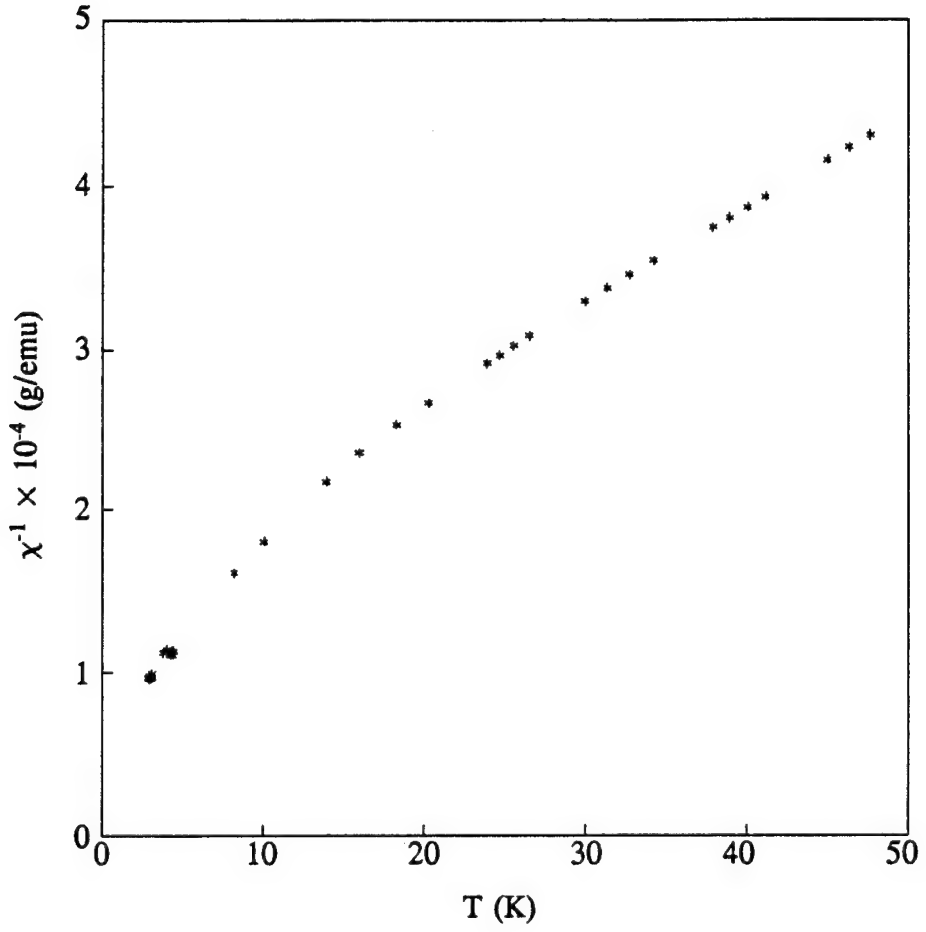
5
4
3
2
1
0
0
10
20
30
40
50
$\chi^{-1} \times 10^{-4}$ (g/emu)
T (K)

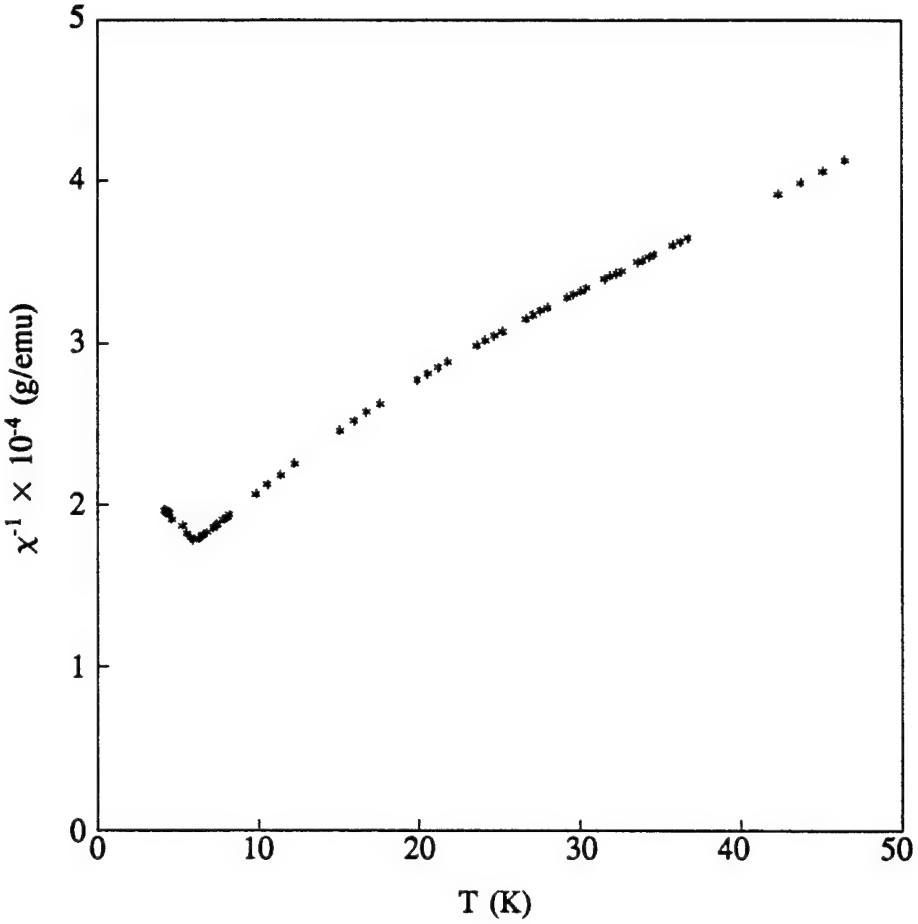
5
4
3
2
1
0
0
10
20
30
40
50
$\chi^{-1} \times 10^{-4}$ (g/emu)
T (K)

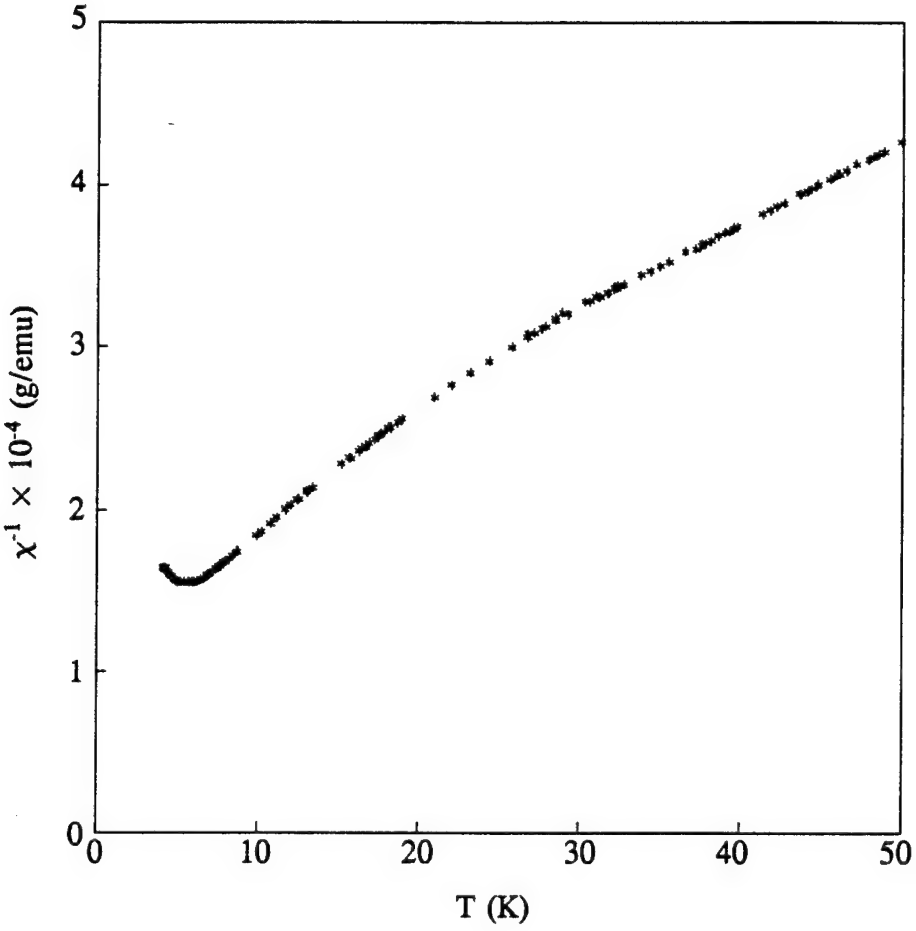
5
4
3
2
1
0
0
10
20
30
40
50
$\chi^{-1} \times 10^{-4}$ (g/emu)
T (K)

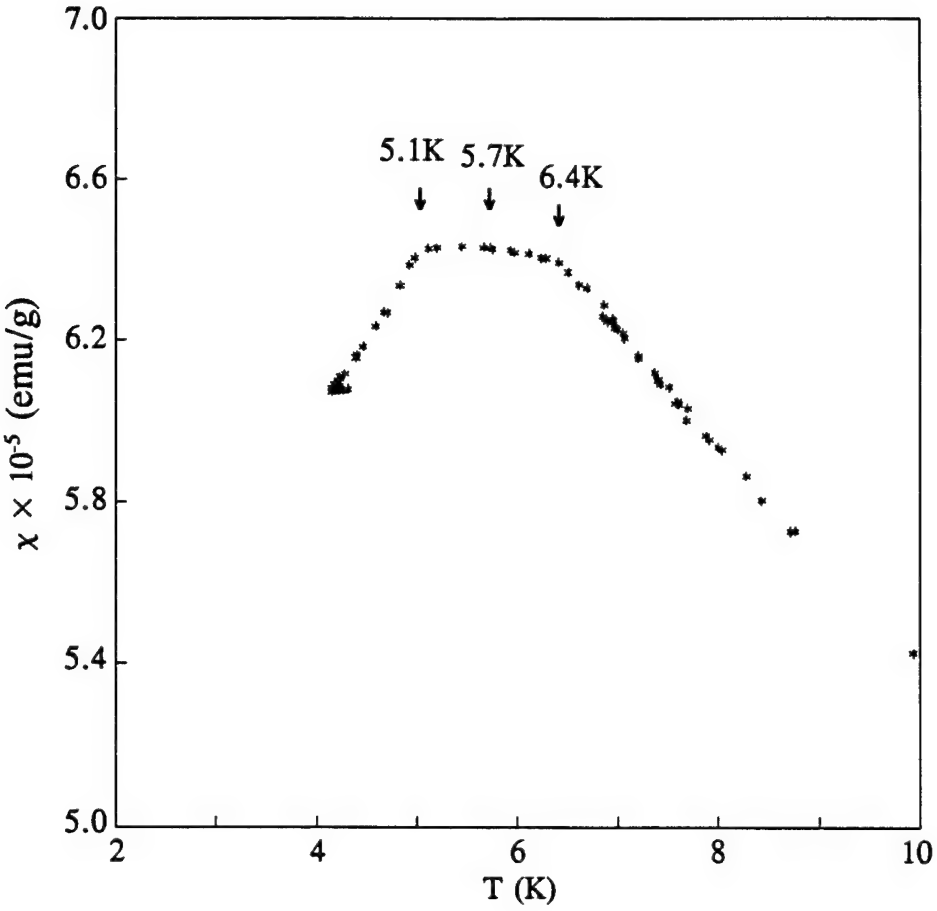
7.0
6.6
6.2
5.8
5.4
5.0
χ × 10⁻⁵ (emu/g)
5.1K
5.7K
6.4K
2
4
6
8
10
T (K)

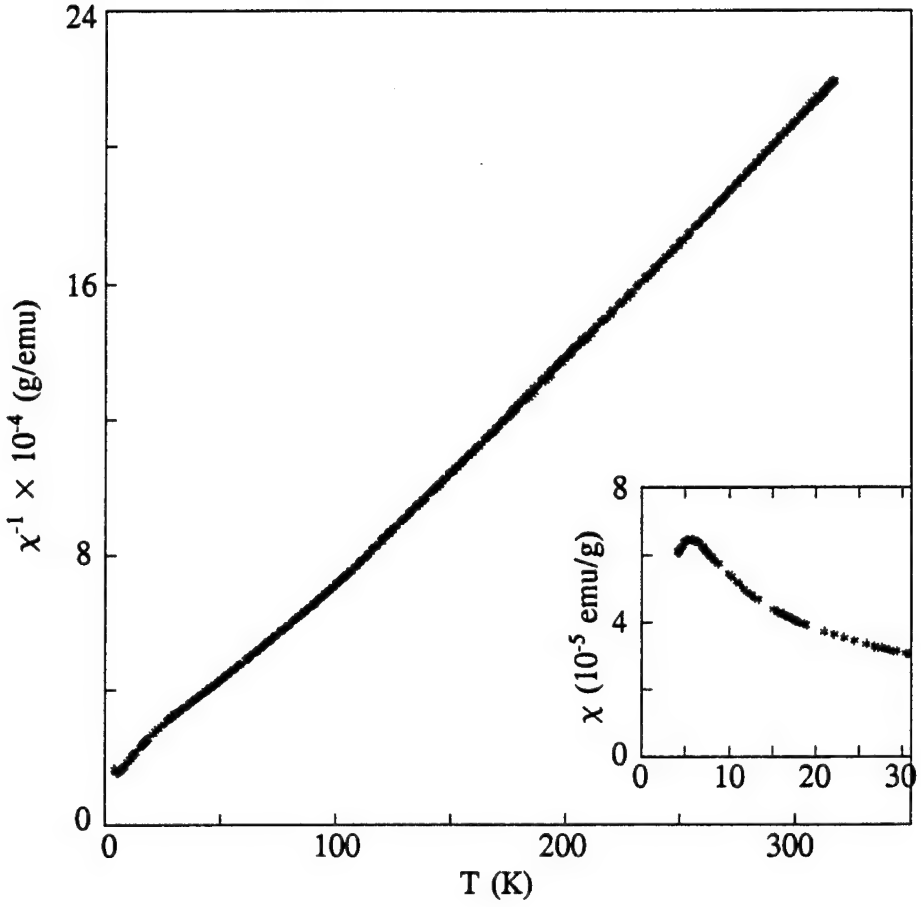
24
16
8
0
$\chi^{-1} \times 10^{-4}$ (g/emu)
0
100
200
300
T (K)
8
4
0
χ (10^{-5} emu/g)
0
10
20
30

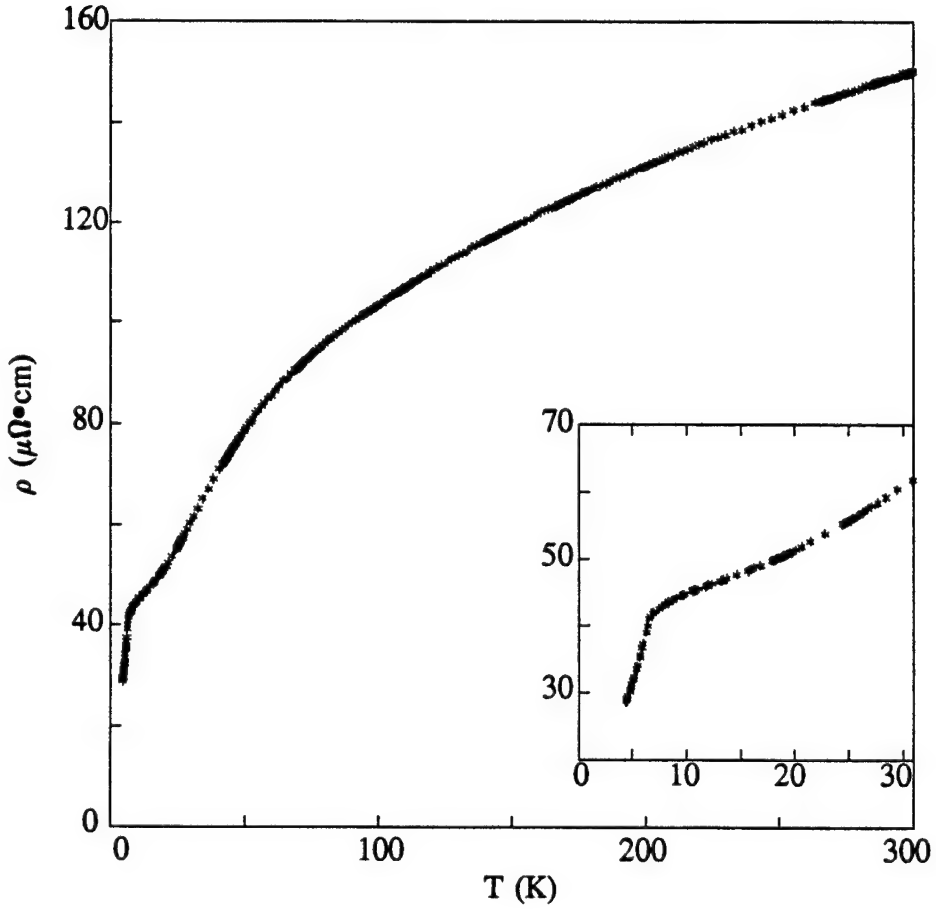
160
120
80
40
0
ρ (μΩ•cm)
0
100
200
300
T (K)
70
50
30
0
10
20
30

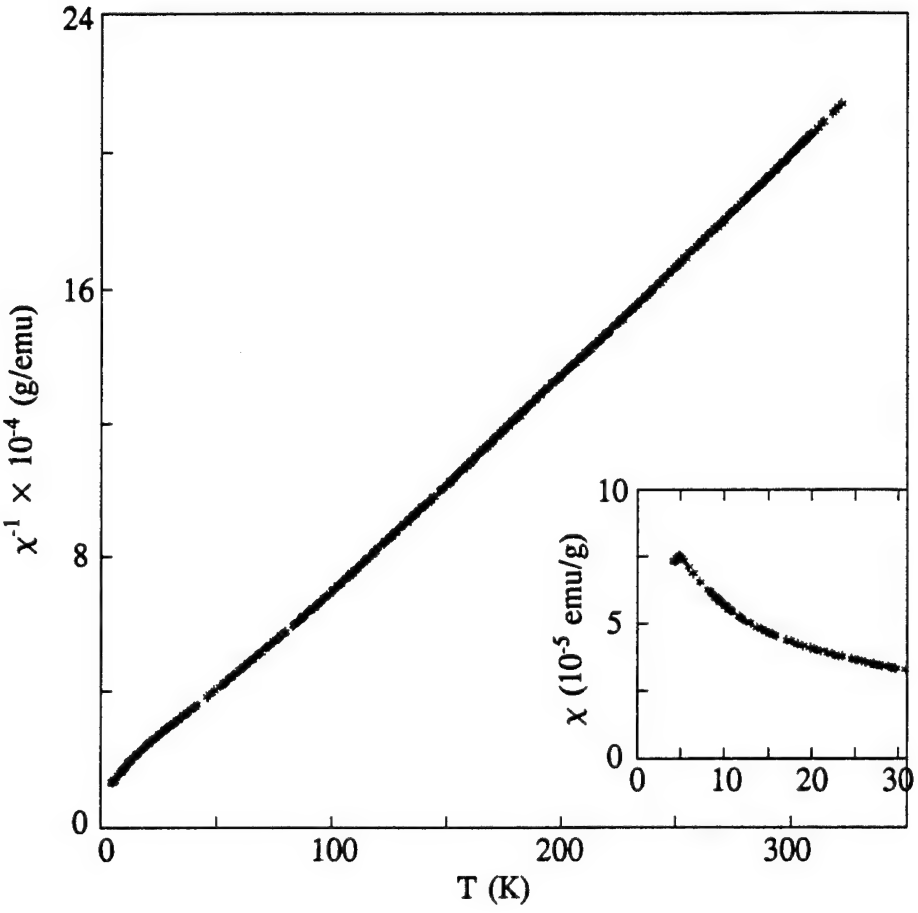
24
16
8
0
$\chi^{-1} \times 10^{-4}$ (g/emu)
0
100
200
300
T (K)
10
5
0
χ (10^{-5} emu/g)
0
10
20
30

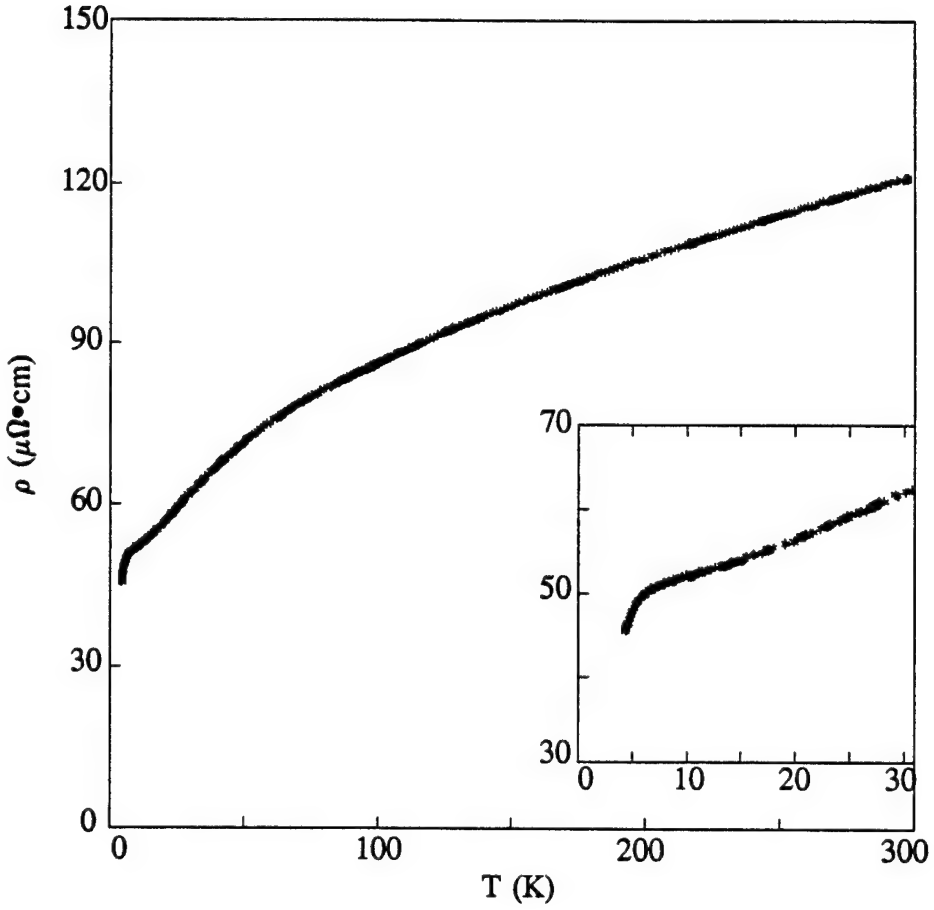
150
120
90
60
30
0
ρ (μΩ•cm)
0
100
200
300
T (K)
70
50
30
0
10
20
30

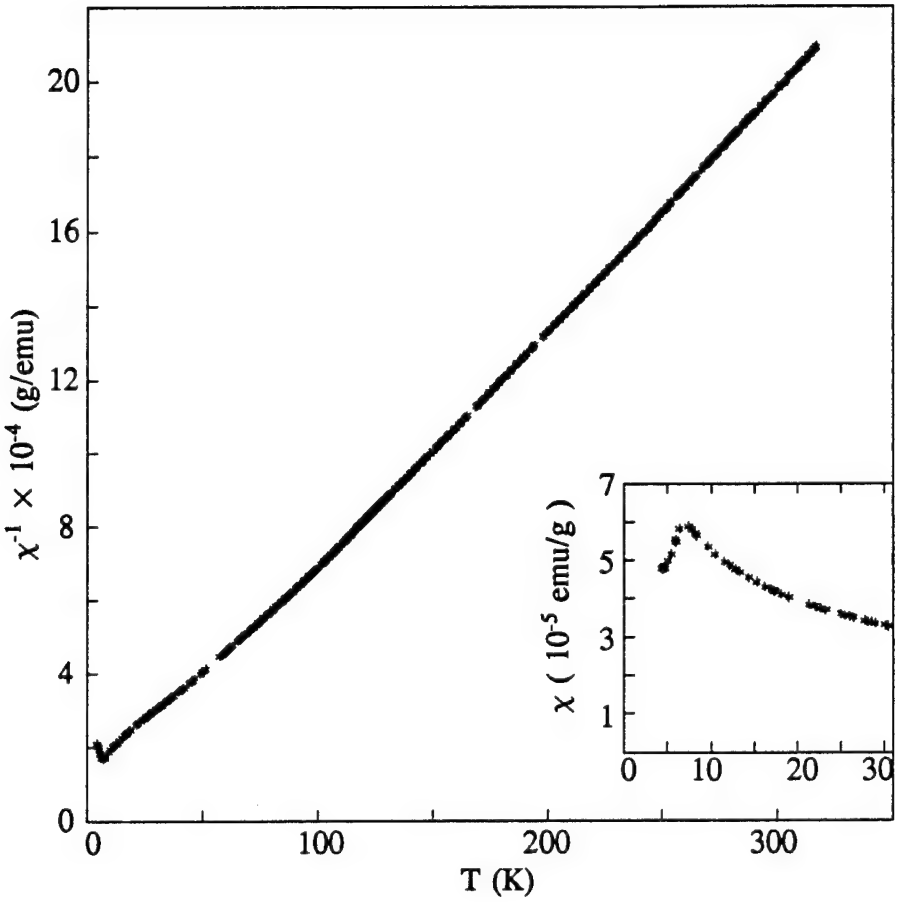
20
16
12
8
4
0
$\chi^{-1} \times 10^{-4}$ (g/emu)
0
100
200
300
T (K)
7
5
3
1
χ (10^{-5} emu/g)
0
10
20
30

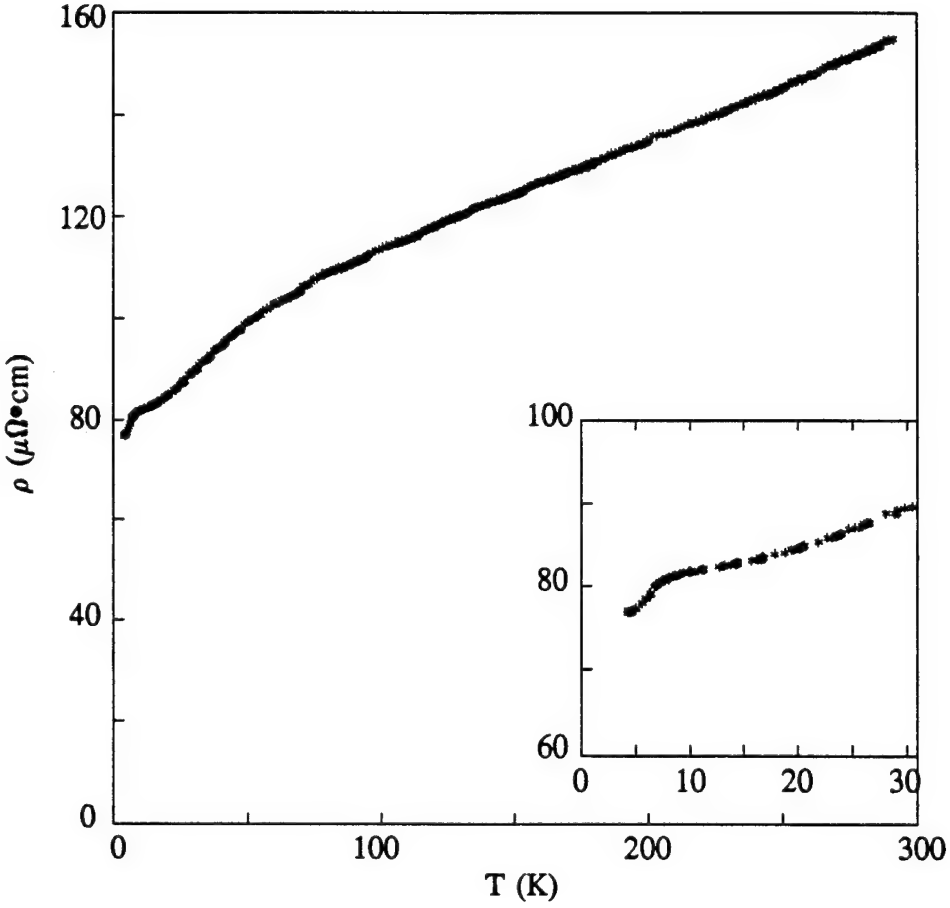
160
120
80
40
0
ρ (μΩ•cm)
0
100
200
300
T (K)
100
80
60
0
10
20
30

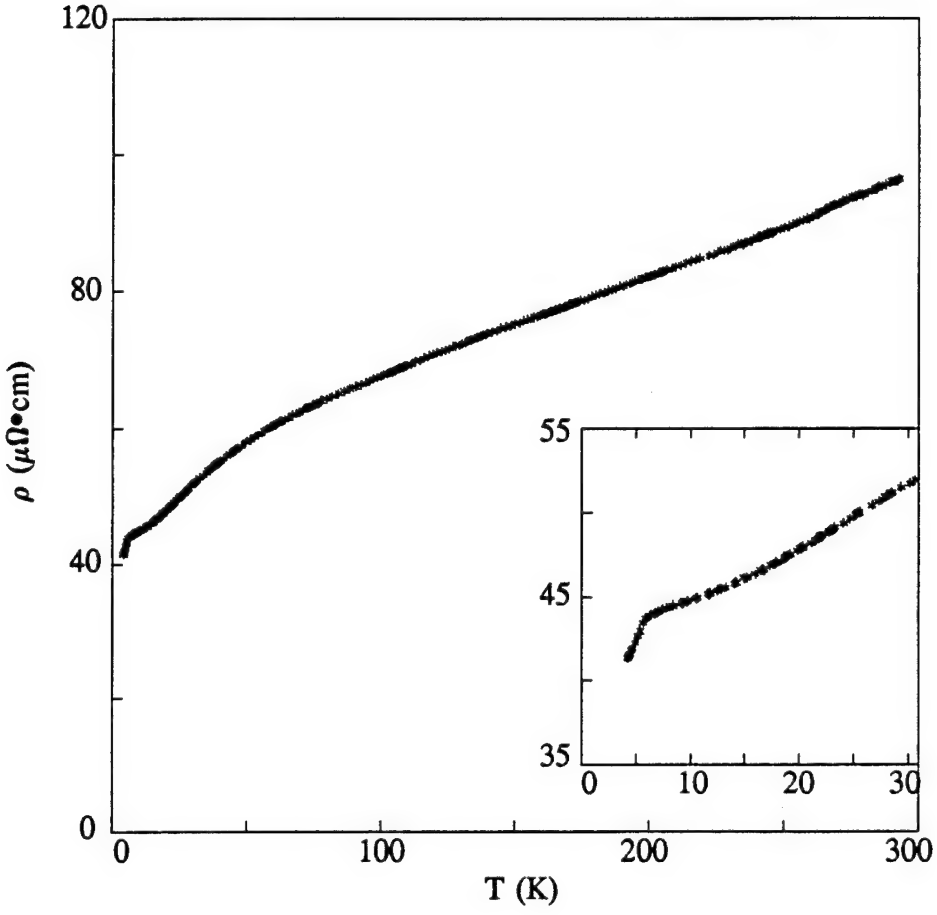
120
80
40
0
ρ (μΩ•cm)
0
100
200
300
T (K)
55
45
35
0
10
20
30

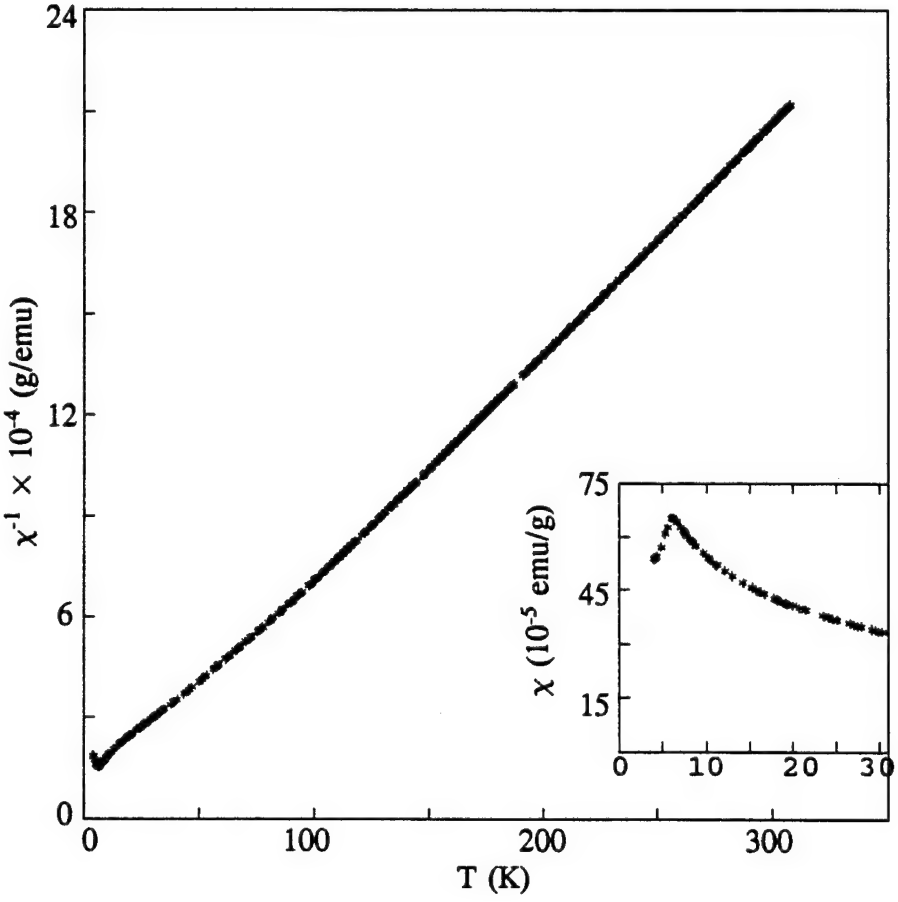
24
18
12
6
0
$\chi^{-1} \times 10^{-4}$ (g/emu)
0
100
200
300
T (K)
75
45
15
χ (10^{-5} emu/g)
0
10
20
30

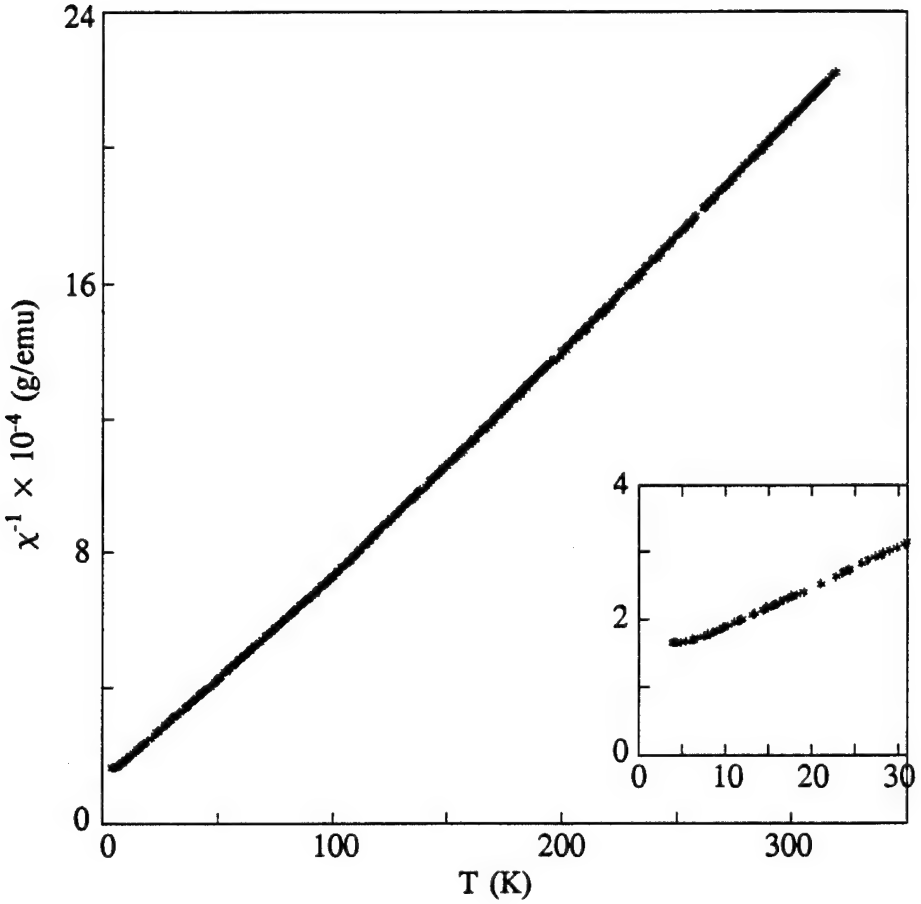
24
16
8
0
$\chi^{-1} \times 10^{-4}$ (g/emu)
0
100
200
300
T (K)
4
2
0
0
10
20
30

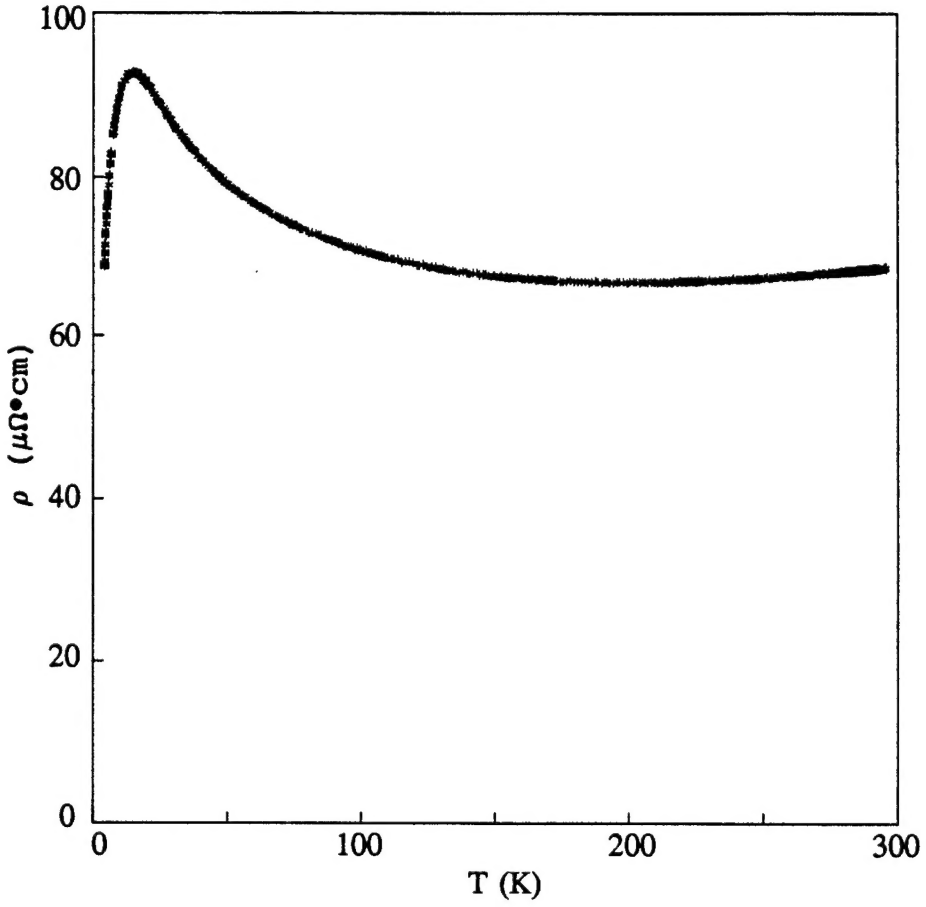
100
80
60
40
20
0
ρ (μΩ•cm)
0
100
200
300
T (K)

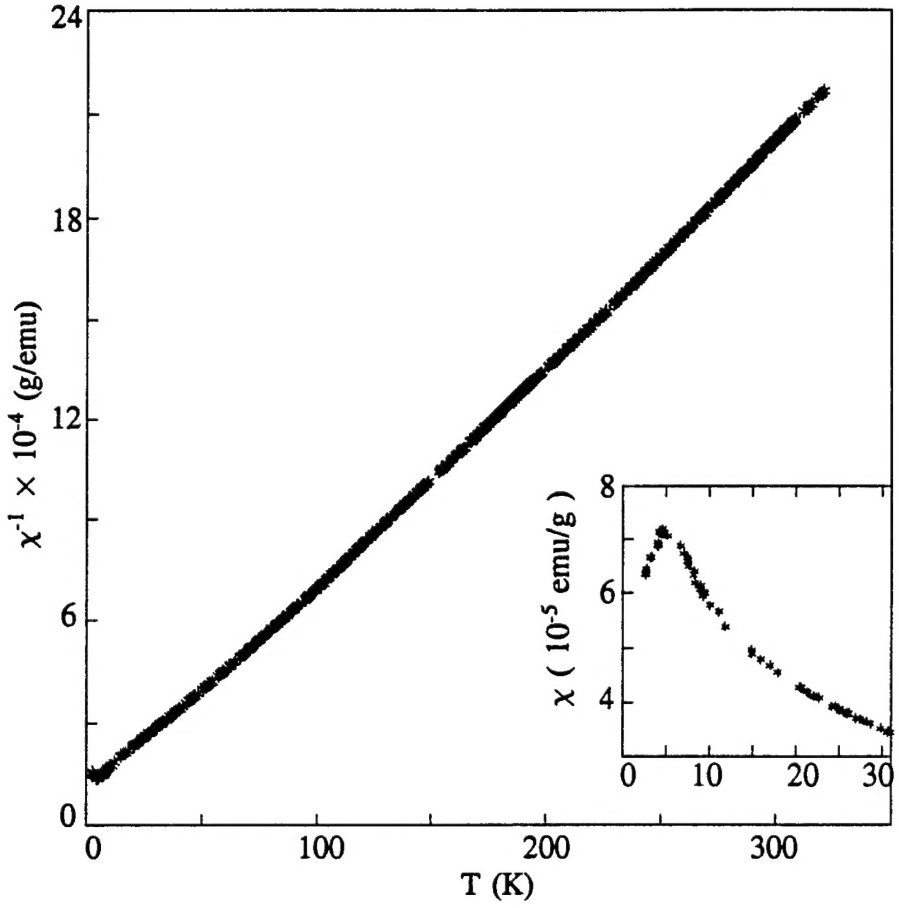
24
18
12
6
0
$\chi^{-1} \times 10^{-4}$ (g/emu)
0
100
200
300
T (K)
8
6
4
χ (10^{-5} emu/g)
0
10
20
30

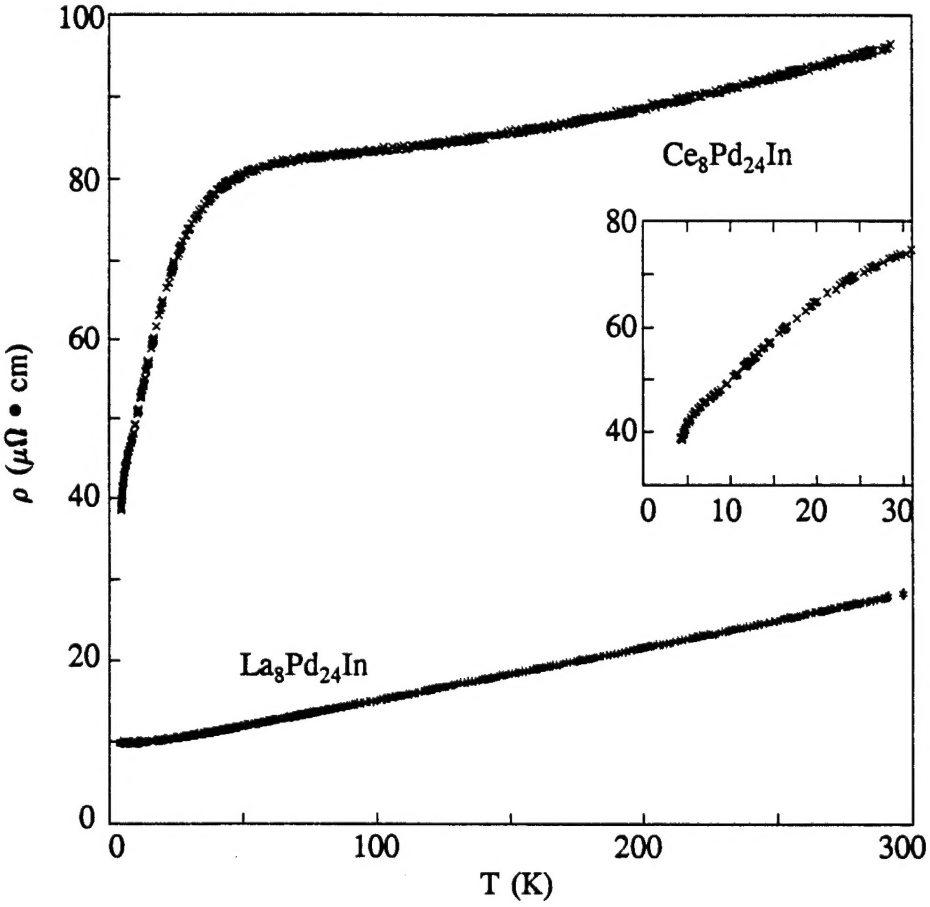
100
80
60
40
20
0
ρ (μΩ • cm)
Ce8Pd24In
La8Pd24In
80
60
40
0
10
20
30
0
100
200
300
T (K)

Technical Report Distribution List

Dr. John C. Pazik (1)*
Physical S&T Division - ONR 331
Office of Naval Research
800 N. Quincy St.
Arlington, VA 22217-5660

Defense Technical Information Ctr (2)
Building 5, Cameron Station
Alexandria, VA 22314

Dr. James S. Murday (1)
Chemistry Division, NRL 6100
Naval Research Laboratory
Washington, DC 20375-5660

Dr. John Fischer (1)

Chemistry Division, Code 385
NAWCWD - China Lake
China Lake, CA 93555-6001

Dr. Peter Seligman (1)
NCCOSC - NRAD
San Diego, CA 92152-5000

Dr. Bernard E. Douda (1)
Crane Division
NAWC
Crane, Indiana 47522-5000

* Number of copies required